Article

Deep Eutectic Solvent as a New Zeta Potential Altering Chemical for Sand Agglomeration

Angelov Tan Yew Ming,* Iskandar bin Dzulkarnain, and Syahrir Ridha

Cite This: ACS Omega 2024, 9, 41321−41333

Read Online

ACCESS | 📊 Metrics & More | 📰 Article Recommendations

ABSTRACT: Fines migration can cause various issues, such as plugging of the sand screen and damage to tubings. There are two chemical sand control methods: consolidation and agglomeration. Consolidation works by injection of a solvent into the formation to harden over time and hold the sand in place, while agglomeration works by altering chemical properties of the sand surface to attract and clump up sand. Various chemicals have been used for research in sand control. Some chemicals for consolidation, mostly resins, have been effective in consolidating sand but may cause

permeability impairment, which will reduce production. Some chemicals for agglomeration such as a polymer with amines have been less effective or are nonbiodegradable. In this work, a novel deep eutectic solvent (DES) and ionic polymer combination as a fines stabilizer is formulated in-house and tested through extensive experimental study. The development of chemicals is based on agglomeration principles which determine the range of zeta potential reduction that can be achieved to destabilize, coagulate, and flocculate the fine particles together with different combinations of DESs and ionic polymers tested systematically using the design of experiment (DoE) method. The chemicals are then tested for compatibility with reservoir fluids in the jar test. The optimized formulation is characterized by thermogravimetric analysis (TGA) for limit of temperature degradation and laser particle size analysis (LPSA) for the extent of particle size. The novelty of this work is the development of a greener and more cost-saving in-house DES and ionic polymer combination as a fines stabilizer chemical, which is effective for both injection or production wells after stimulation or enhanced oil recovery (EOR) treatments. Due to the tunable nature of the DES, the formulated chemical can be tailored for various reservoir conditions to cater to specific requirements.
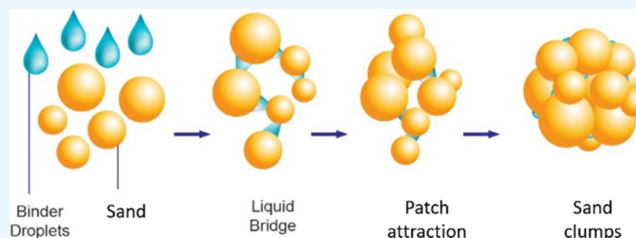
1. INTRODUCTION

Sand production has been an unavoidable issue in the oil and gas industry. It is the delocalization of sand particles from the rock formation when the formation strength is weaker than the stress around the wellbore. Sand production will pose various issues to production operations such as plugging and erosion to equipment.[1,2] There are two categories of sand control methods, namely, mechanical and chemical methods. The mechanical method uses sand screens and gravel packs to retain sand; they are made of wires of different sizes made into a screen to prevent sand grains from entering the wellbore. There are two methods of chemical sand control: consolidation and agglomeration. The consolidation method works by injecting a solvent such as a resin into the rock formation, followed by a hardener to solidify the solvent to hold the sand in place. It will then be followed by perforating the consolidates to further create channels for fluid flow.[3] Such methods of sand control have posed problems such as permeability impairment due to resin particles occupying pore spaces[4] and timing estimations as the resin and hardener must be premixed before injection and the hardening takes place immediately. The agglomeration method commonly uses polymers or amine compounds through a bridging effect to

bind sand grains and form bigger clumps to be retained on the sand screen. Agglomeration methods that use ionic liquids paired with polymers have received more attention for research. Some recent studies have used zeta potential altering solutions (ZPASs) with a polymer, but they might be less durable or nonbiodegradable. Agglomeration can be promising, but the efficiency can only achieve a 12-month period of sand-free production.

The zeta potential is an important parameter in particle agglomeration. The zeta potential is the potential difference between the slipping plane of a surface and that of the surrounding fluid. A high value of either the positive or negative zeta potential indicates that the particles will repel each other and hence the tendency for agglomeration is highly unlikely, while to form agglomerates, the zeta potential value

Table 1. DoE Parameter Design

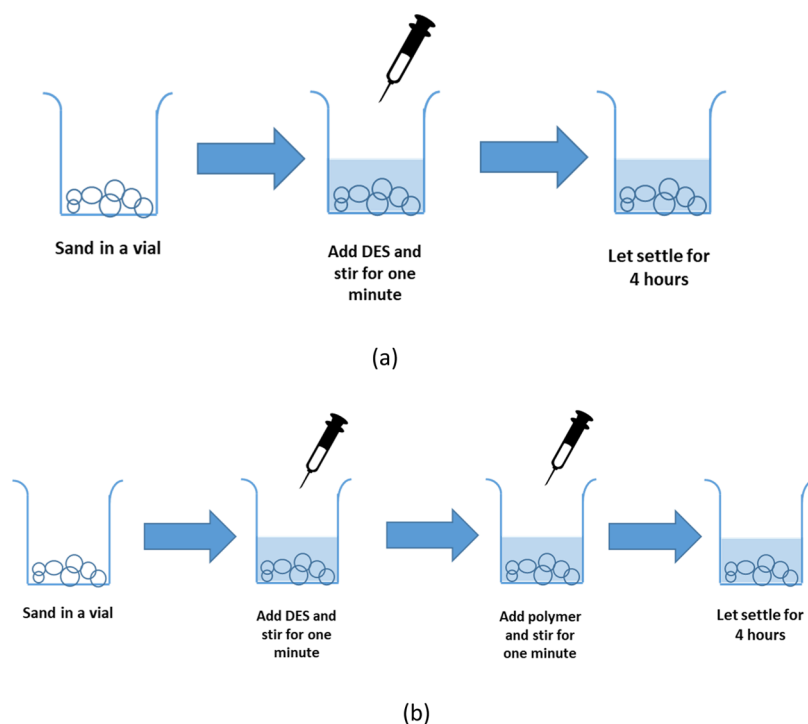| factor	name	units	type	minimum	maximum	coded low	coded high
A	brine		categoric	NaCl	MgCl$_2$		
B	DES conc.	mg/L	numeric	5000.00	10000.00	$-1 \leftrightarrow 5000.00$	$+1 \leftrightarrow 10000.00$
C	polymer conc.	mg/L	numeric	250.00	500.00	$-1 \leftrightarrow 250.00$	$+1 \leftrightarrow 500.00$
D	polymer dosage	mL	numeric	1.00	2.00	$-1 \leftrightarrow 1.00$	$+1 \leftrightarrow 2.00$
E	temperature	°C	numeric	25.00	90.00	$-1 \leftrightarrow 25.00$	$+1 \leftrightarrow 90.00$
F	polymer type		categoric	AN	FO		

Figure 1. Illustration of the jar test for (a) the DES only and (b) the DES and the polymer.

should be within ± 5 mV. These surface charges can be altered and it depends on several factors such as the charge density, ionic strength of the solvent, temperature, and pH.[5] Sand surfaces are known to possess a charge of -30 mV.[6] Charge neutralization is one of the most common mechanisms in promoting agglomeration. Charge neutralization can be achieved by exposing the sand particles to a positively charged solvent to destabilize the surface charge and cause rapid agglomeration. In order to form stable colloidal systems, the zeta potential must be altered to become more positive.[7]

Polymer bridging is a process in which a polymer is adsorbed into one or more particles and will bind them together. This process usually occurs when a high-molecular-weight polymer is added.[8] Typically, high-molecular-weight polyacrylamide is used for this reaction. The bridging occurs due to the attractive forces between the polymer and the particle surfaces to form colloidal systems. In a colloidal system, solvents such as polymers are added to the sand; the polymer will interact with the particles to form attractive forces. This reaction will result in sand particles being attracted to each other, thus forming agglomerates. Patch attraction will occur when agglomerates are bound by the polymers and they form larger and more stable clumps. Polymer additives such as cross-linkers can be added into a polymer system to enhance the reaction.[9,10] Cross-linkers range from organic to inorganic compounds such as acetic acid, ammonium sulfate, hydro-

chloric acid, etc. Studies have shown that charged polymers even at low concentrations, Al-Risheq[11,12] using 10−35 mg/L and M. Fauzi (2020)[6] using 100 mg/L, are able to increase the size distribution of sand and bentonite effectively.

The sand agglomeration solvents such as polymers, ionic liquids, and deep eutectic solvents have a certain range of operating temperature for them to be chemically stable. Since these solvents are held together by ionic bonds or hydrogen bonds, certain high reservoir temperatures will cause the bonds between particles to break down and lose its effects.[13,14] The temperature effect on solvents can be assessed by running through thermogravimetric analysis (TGA). TGA will show that with an increase in temperature, the stability of the solvents begins to decline and the temperature limit where the bonds of the solvent particles begin to disintegrate will be determined.

New studies are aimed toward deep eutectic solvents (DESs), which have been widely studied in the past decade in the field of pharmaceuticals and biotechnology as a medium to promote the formation of suspensions by altering the surface charge of particles.[15−21] DESs are made from a hydrogen bond acceptor (HBA) and a hydrogen bond donor (HBD) that are relatively common materials such as choline chloride as HBAs and urea, glycine, and many more as HBDs. They are mostly nontoxic,[22] inexpensive to acquire, and can be manufactured easily. Most DESs can be tuned to cater to
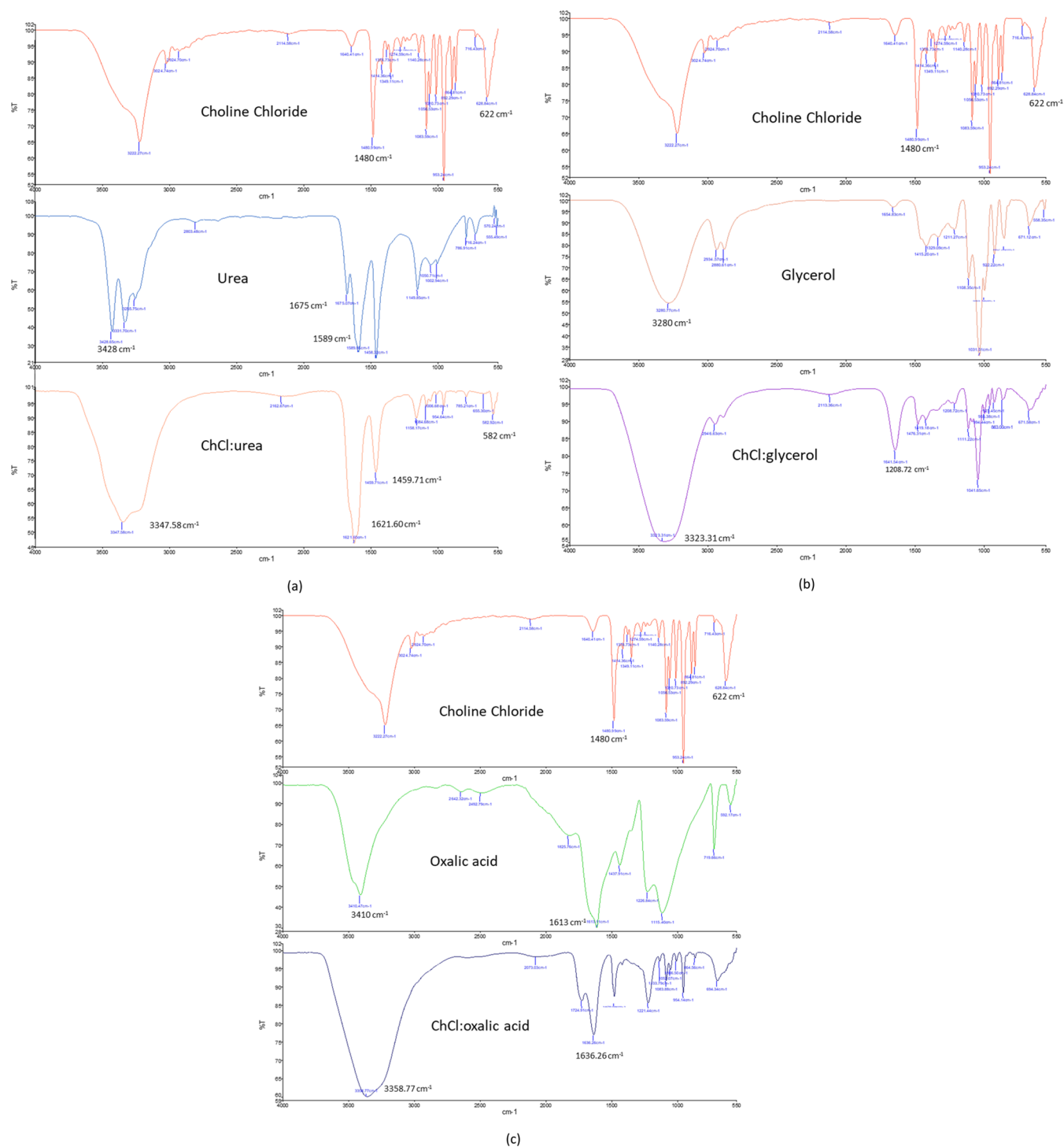
Figure 2. FTIR of (a) choline chloride, urea, and ChCl:urea, (b) choline chloride, glycerol, and ChCl:glycerol, and (c) choline chloride, oxalic acid, and ChCl:oxalic acid.

specific or desired situations, such as changing the ratio of HBAs to HBDs to have different eutectic points and melting points.[23−25] In the early 2010′s, the usage of DESs has been heavily focused on microextraction operations such as water treatment, where they were proven to be highly effective in flocculating waste materials.[17,18] Studies of application in the oil and gas industry have started to gain popularity since 2015. Current studies have been applied in drilling mud additives due to their inhibition properties and for wettability alteration and interfacial tension (IFT) reduction for enhanced oil

recovery (EOR) purposes.[7,25−29] In this study, the DES functions to reduce the zeta potential of the sand to promote better agglomeration, as a zeta potential of ±5 mV is the range where particles start to destabilize and form agglomerates. The ionic polymer then binds the sand together through polymer bridging to form bigger clumps.

This study was conducted to investigate the effect of the ion composition of brine (monovalent and divalent) and temperature on the effectiveness of agglomeration with the combination of a DES and an ionic polymer. After that, the
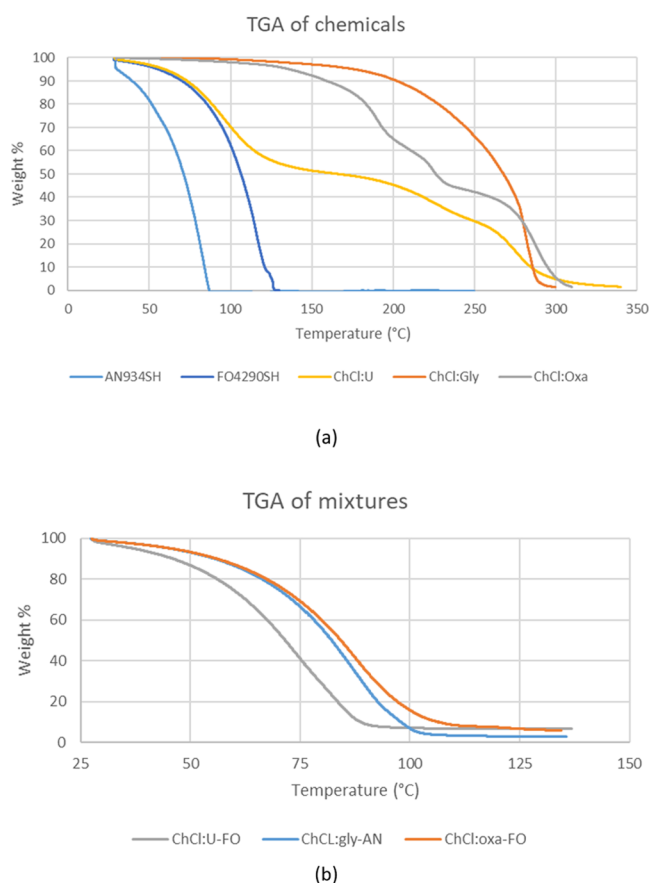
(a)

(b)

Figure 3. TGA of (a) individual chemicals and (b) the DES and polymer mixtures.

Table 2. XRD Analysis Table

sample	quartz	feldspar	kaolinite	muscovite	total
sand	74	11	0	15	100

factors such as the DES concentration, polymer concentration, polymer dosage, and temperature were optimized with the response surface methodology (RSM). Three types of DESs were used, which are choline chloride-urea, glycerol, and oxalic acid and two types of polymers, which are anionic (AN934SH) and cationic (FO4290SH) polymers, This study has investigated the combinations and chosen the most effective DES−polymer combination.

2. METHODOLOGY

2.1. Preparation of Materials. The sand sample used was silica sand with the size ranging from 100 to 150 μm. Choline chloride (ChCl, Sigma-Aldrich, >98%), urea (Merck), glycerol (Fisher, >99%), oxalic acid (Sigma, >98%), methylenebis-(acrylamide) (Sigma-Aldrich, 99%), and potassium persulfate (Sigma-Aldrich, 99%) were purchased from Avantis Laboratory Supplies. The anionic polymer AN934SH, which is a copolymer consisting of acrylamide (C_3H_5NO) and sodium acrylate ($C_3H_3NaO_2$), and the cationic polymer FO4290SH, which is a copolymer consisting of acrylamide (C_3H_5NO) and dimethylaminoethyl acrylate ($C_7H_{13}NO_2$), were supplied by SNF France.

Prior to preparation of the DES, choline chloride and urea were dried under vacuum. The weight ratio of ChCl to HBD was measured using an electronic weight balance. The

eutectic solvents were prepared according to the steps given by Abbott et al.[23] Both ChCl and urea were weighed and mixed in a 1:2 mol ratio in a beaker. The beaker was heated to 80 °C and stirred at 250 rpm for 30 min until a homogeneous liquid was obtained. The steps were repeated similarly for all DESs with their respective molar ratios. The polymers were prepared according to 250 and 500 mg/L concentrations. This is because increasing concentrations can result in high viscosity, which will affect the rheology of the formulation. The potassium persulfate solution as an initiator was dissolved in hot water in a 500 mg/L concentration, and the polymer and methylenebis(acrylamide) (50 mg) were added into the mixture and stirred for 40 min until it thickened.

2.2. Preliminary Testing. Fourier transform infrared (FTIR) spectroscopy is an analytical technique used to identify various bonds such as hydrogen, hydroxyl, C−H, and many other bonds in organic or inorganic compounds. FTIR analysis uses infrared light to scan the chemicals through a span of wavelengths, and specific bonds will be detected from the peaks shown by certain wavelengths. The FTIR spectra of choline chloride, urea, glycerol, oxalic acid, and the prepared DES were generated using a PerkinElmer Frontier 01 FTIR spectrometer. The spectrum was recorded through a resolution of 4 cm^{-1} over a wavenumber ranging from 550 to 4000 cm^{-1} at room temperature and the attenuated total reflectance (ATR) method was used to capture the bonds present in each compound and the hydrogen bonds that have been formed in the DES. Four scans were performed and the average was obtained by the software.

The X-ray diffraction (XRD) analysis can be used to identify crystalline and noncrystalline structures present in the sand sample. The sand used was silica sand of 100−150 μm. Clay mineral identification is vital toward further analysis as water and brine in the chemicals may cause the clay to swell and affect the overall efficiency of the agglomeration mechanism. The XRD patterns were obtained using a benchtop X-ray diffractometer (D2 Phaser) operating at 45 kV and 40 mA with Cu Kα radiation (λ = 1.54059 Å). The 2θ interval used was from 0−90°. The step size used was 0.026 Å/s over 100 s. Bragg's equation was then used to find the interlayer spacing. Highscore 3+ COD software was used to match the peaks of mineral phases. The Inorganic Crystal Structure Database (ICSD) was used to identify the minerals. Rietveld analysis was used to quantify the mineral phases in the sample.

The Malvern Zetasizer nano ZSP was used to analyze the zeta potential as well as the particle size distribution of the sand particles. For sand agglomeration experiments to be deemed successful, it is necessary to determine the size of the lumps after a certain solvent has been added. The most common test done to determine particle size distribution is by running it through a laser particle size analyzer (LPSA). LPSA results will show a normal distribution graph showing the volume percentages of various size populations, such as d_{10}, d_{50}, and d_{90}, that have been detected. d_{10} represents the smallest particle size as it shows 10% of the distribution retained in the corresponding mesh of a distribution, d_{50} represents 50% of the distribution retained in the correspond-ing mesh of a distribution, and d_{90} represents the biggest particle size as it shows 90% of the distribution retained in the corresponding mesh of a distribution. The sand together with the liquid was loaded into the capillary cell with 1 mL at most. The laser was set at a single wavelength of 633 nm. The particle size and zeta potential were calculated by the software.
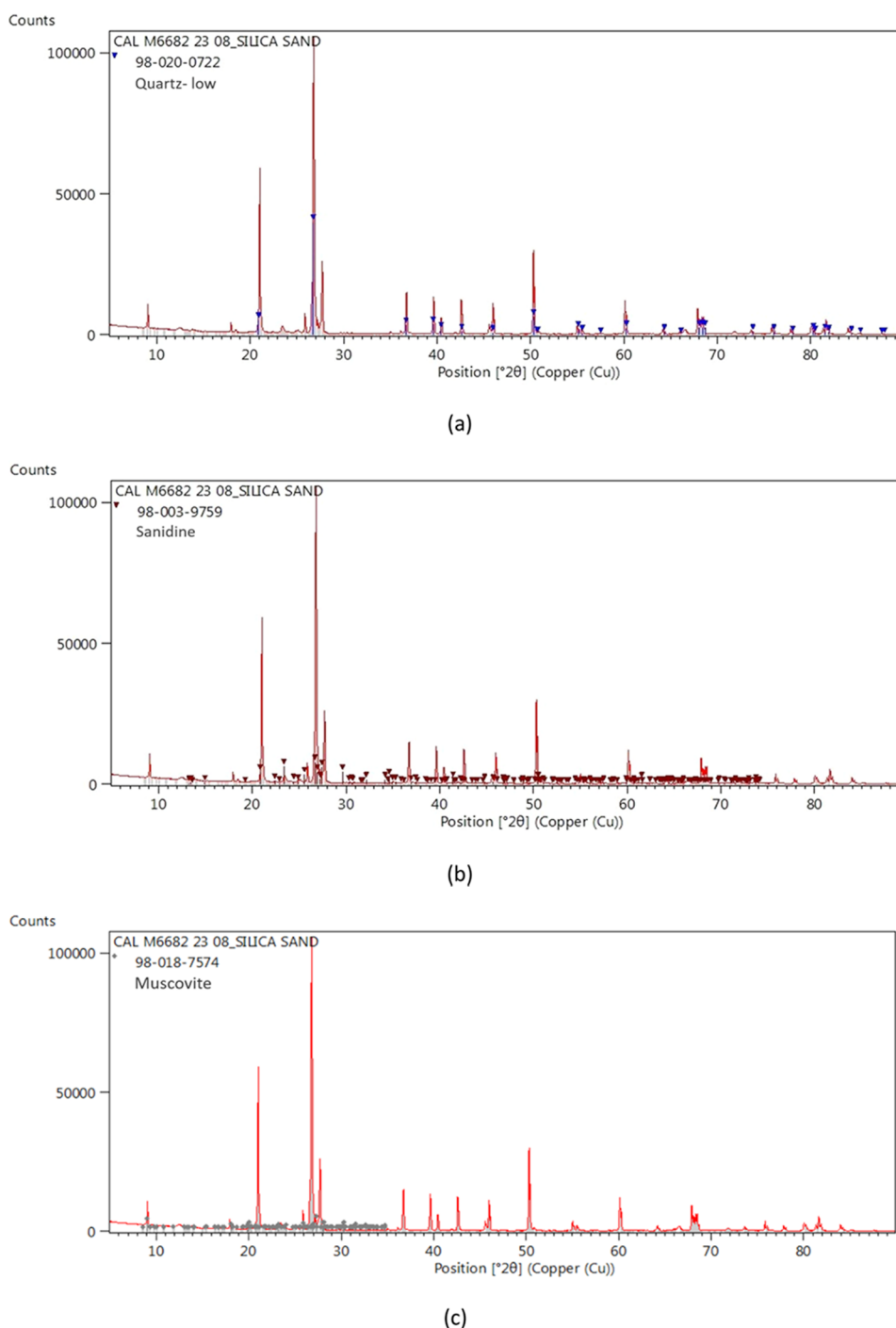
(a)

(b)

(c)

Figure 4. XRD results of (a) quartz, (b) sanidine, and (c) muscovite.

Thermogravimetric analysis (TGA) was performed using the PerkinElmer STA6000 thermal analyzer. The liquid sample (20 mg) was placed on a ceramic crucible and loaded into the machine. The temperature range was set from 25−500 °C with a heating rate of 10 °C/min. The sample was burned under nitrogen gas. The results were then generated by the software and plotted on a graph.

2.3. Design of Experiment (DoE). The design of experiment (DoE) was implemented to come up with a series of tests and obtain a relationship for optimization purposes. In this experimental design, Design Expert 13 was used to model the six variables, which are the type of brine, type of DES, DES concentration, polymer concentration, polymer dosage, and temperature, while the three responding variables are the particle size, zeta potential, and turbidity. The Box-Behnken design (BBD) was used to generate the limits of variables, as shown in Table 1. By the input of the range of each variable, the appropriate amount of runs to be executed was generated by the software. In this study, the 2^6 fractional factorial was used to generate 16 runs for each type of DES, adding up to 48 runs in total. The software was able to verify and analyze the relationship between the inputs on a plot to observe the relation toward the responding variables. Next, an ANOVA table was provided by the software to confirm the level of
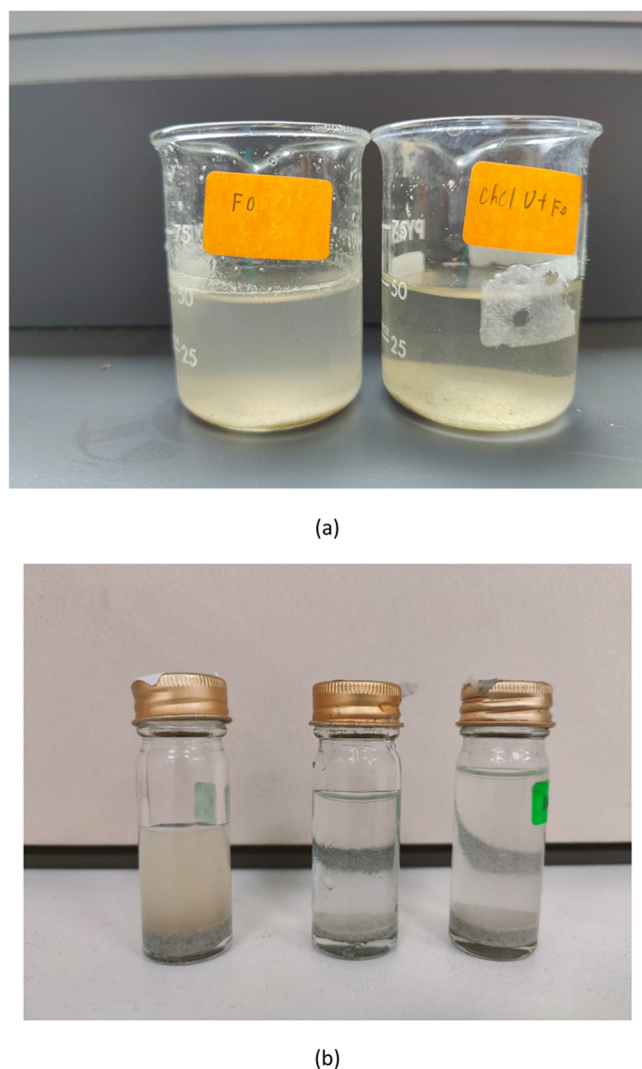
(a)

(b)

Figure 5. (a) Jar test with FO4290SH on the left and ChCl:urea + FO4290SH on the right. (b) Jar test with ChCl:oxa on the left, with AN934SH in the center and with FO4290SH on the right.

Table 3. Effectiveness of Individual Chemicals on Agglomeration

chemicals	size (μm)	zeta potential (mV)	turbidity (NTU)
FO4290SH	183.4	−15.6	15.72
AN934SH	176.8	−18.45	20.67
ChCl:U	131.8	−12.12	5.22
ChCl:gly	145.7	−10.8	30.56
ChCl:oxa	146.3	−9.15	2.17

significance of each variable toward the responding variable, and the correlation coefficient R^2 was also provided to prove the confidence level of the analysis.[30−32] R^2 in the DoE is the determination coefficient as a correlation coefficient is used for nonintentional variation of the independent factors or variables. After that, an equation was generated by the software based on the variables, and this was used to optimize the best combination of parameters to achieve the best results. Finally, the solutions for the optimized parameters were generated through numerical optimization.

2.4. Agglomeration Jar Test. The DES in brine solutions was prepared by mixing the DES in 30000 ppm NaCl brine.
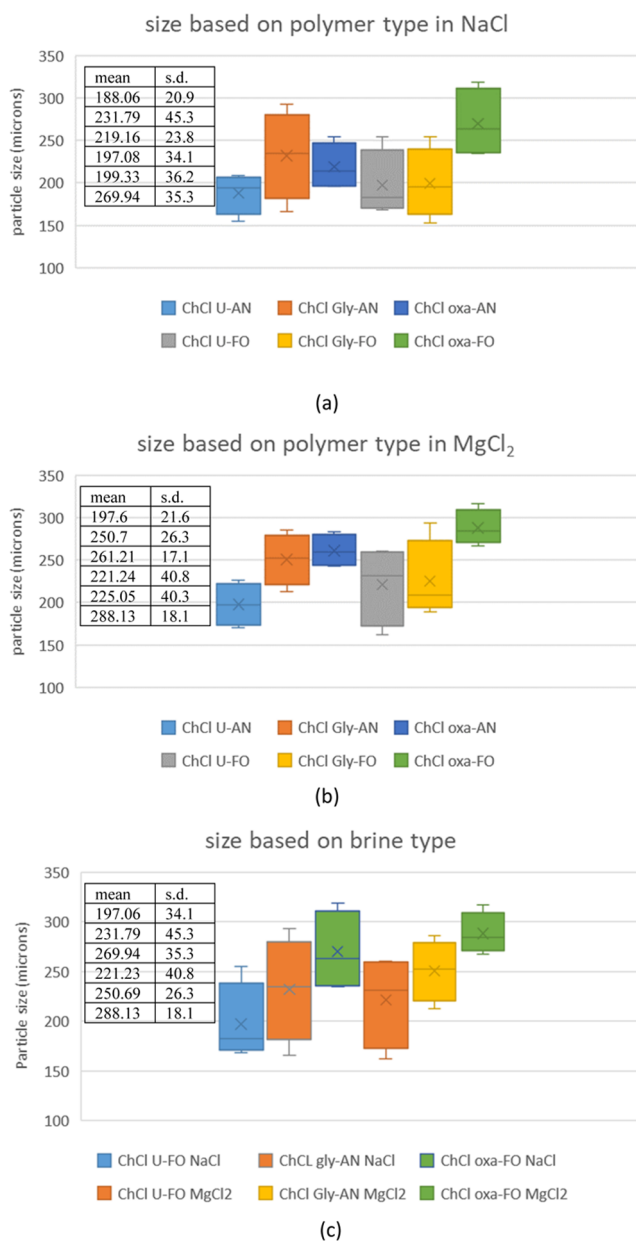

(a)

(b)

(c)

Figure 6. Box and whisker plot for the particle size based on (a) the polymer type in NaCl, (b) the polymer type in MgCl$_2$, and (c) the brine type.

The mixture was stirred under 500 rpm at 50 °C for 10 min. The polymer solution was prepared by mixing according to the concentration from the DOE and stirred under 200 rpm at ambient condition for 10 min until a homogeneous liquid was obtained.

The jar test was performed in a vial under ambient conditions to observe the agglomeration mechanism. Figure 1a shows the jar test with the DES alone. Five g of sand has been prepared and placed into the vial. Twenty mL of DES solution was added into the vial and left for 4 h. The sample of sand was taken out and loaded into a Malvern Zetasizer to measure the zeta potential and particle size distribution. Figure 1b shows the jar test with the DES and the polymer. The steps were also repeated with the DES in brine and polymer solution to obtain the most suitable composition. The polymer concentration was changed from 250 to 500 ppm and the
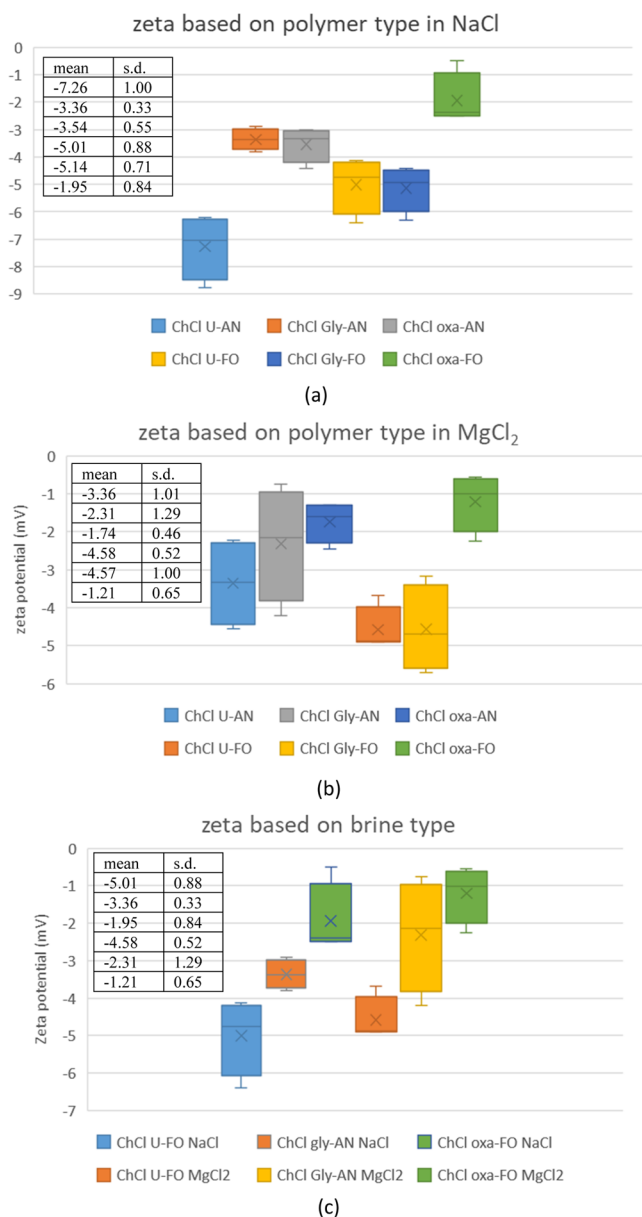
zeta based on polymer type in NaCl

mean	s.d.
-7.26	1.00
-3.36	0.33
-3.54	0.55
-5.01	0.88
-5.14	0.71
-1.95	0.84

ChCl U-AN ChCl Gly-AN ChCl oxa-AN
ChCl U-FO ChCl Gly-FO ChCl oxa-FO

(a)

zeta based on polymer type in MgCl$_2$

mean	s.d.
-3.36	1.01
-2.31	1.29
-1.74	0.46
-4.58	0.52
-4.57	1.00
-1.21	0.65

ChCl U-AN ChCl Gly-AN ChCl oxa-AN
ChCl U-FO ChCl Gly-FO ChCl oxa-FO

(b)

zeta based on brine type

mean	s.d.
-5.01	0.88
-3.36	0.33
-1.95	0.84
-4.58	0.52
-2.31	1.29
-1.21	0.65

ChCl U-FO NaCl ChCl gly-AN NaCl ChCl oxa-FO NaCl
ChCl U-FO MgCl2 ChCl Gly-AN MgCl2 ChCl oxa-FO MgCl2

(c)

Figure 7. Box and whisker plot for the zeta potential based on (a) the polymer type in NaCl, (b) the polymer type in MgCl$_2$, and (c) the brine type.

Figure 8. Pareto chart of the particle size for ChCl:oxalic acid.

Predicted vs. Actual

Std. Dev.	11.93
Mean	248.98
C.V. %	4.79
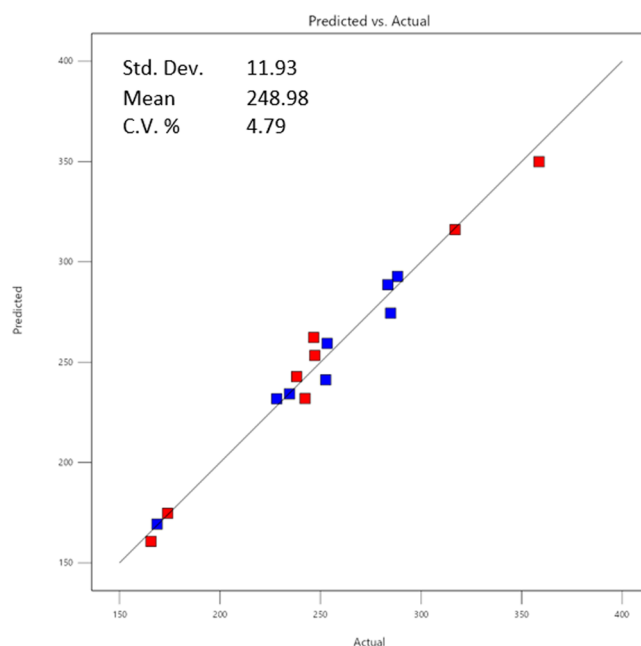
Figure 9. Predicted vs actual values of the particle size of ChCl:oxalic acid.

dosage was changed from 1 to 2 mL to observe the effects on the agglomeration mechanism.

3. RESULTS AND DISCUSSION

3.1. Preliminary Results. *3.1.1. Fourier Transform Infrared (FTIR) Spectroscopy.* The Fourier transform infrared (FTIR) spectroscopy results were used to confirm the formation of bonds in the respective DES, as shown in Figure 2. For the ChCl:urea DES, the characteristic peak of −NH$_2$ shifted from 3428 to 3347 cm^{-1} and broadened to confirm the formation of hydrogen bonds, the C=O shifted from 1675 and 1589 to 1621 cm^{-1} and appeared at 582 cm^{-1} and CH$_2$ that shifted from 1480 to 1459 cm^{-1} can be seen in the DES to confirm its formation.[14,25] For the ChCl:glycerol DES, the characteristic peak of −OH shifted from 3280 to 3323 cm^{-1} and broadened to confirm the formation of hydrogen bonds and the appearance of the peak at 1208 cm^{-1} represents the
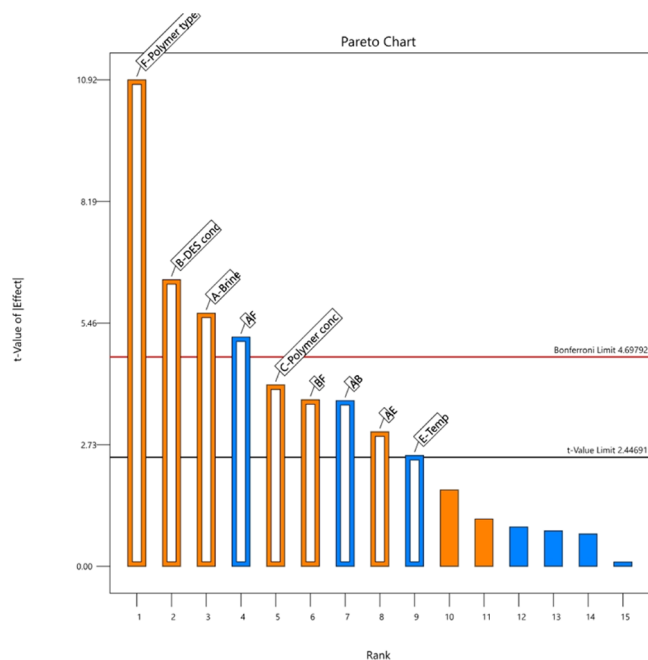
bending of C−O. For the ChCl:oxalic acid DES, the characteristic peak of −OH shifted from 3410 to 3358 cm^{-1} and broadened to confirm the formation of hydrogen bonds, the C=O shifted from 1613 to 1636 cm^{-1} to confirm its formation.

3.1.2. Thermogravimetric Analysis (TGA). Thermogravimetric analysis (TGA) is important to determine the thermal stability and melting point of chemicals to assess the suitability at high reservoir temperatures. Figure 3 shows the TGA of 3 DESs and both ionic polymers. All 3 DESs have a very high thermal stability in which they started to break down at temperatures above 100 °C. ChCl:U started to break down at 50 °C; the breaking down decreased, and it reached 50% at
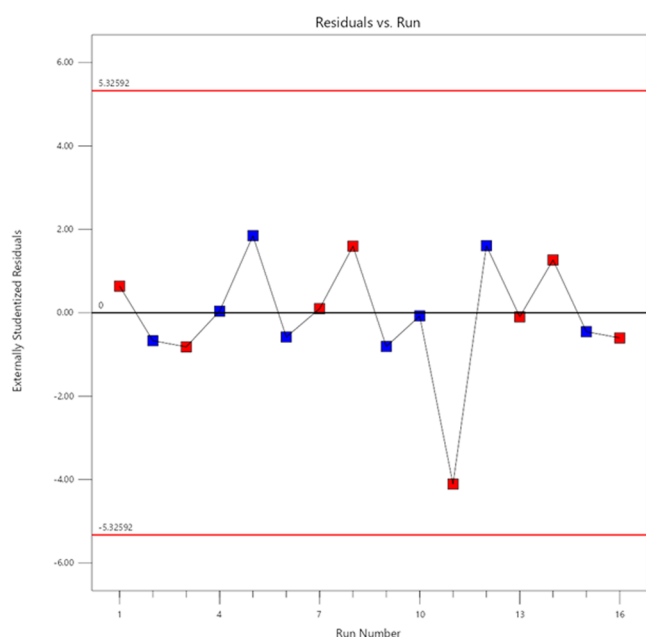
Figure 10. Residual vs run values of the particle size of ChCl:oxalic acid.

160 °C and totally decomposed at 350 °C. ChCl:oxalic acid started to break down at 100 °C; it reached 50% at 230 °C and totally decomposed at 320 °C. ChCl:gly started to decompose at 130 °C; the breaking down increased, and it reaches 50% at 220 °C and completely decomposed at 300 °C. Both ionic polymers have a low thermal stability in which AN934SH started to break down at 30 °C and had totally broken down at 90 °C. FO4290SH started to break down at 50 °C and had totally broken down at 125 °C. All 3 DESs have a high thermal stability and can withstand a high reservoir temperature, while the ionic polymers have a low thermal stability and will break down at a temperature below the reservoir temperature.

Figure 3b shows the thermal decomposition of the DES and polymer mixtures. ChCl:U-FO reached 50% at 70 °C and totally decomposed at 90 °C. ChCl:gly-AN reached 50% at 80 °C and totally decomposed at above 100 °C. ChCl:oxa-FO reached 50% at 90 °C and totally decomposed at above 100 °C. Hence, ChCl:oxa-FO and ChCl:gly-AN have a similar performance at high temperatures.

3.1.3. X-ray Diffraction (XRD). The mineralogy of the sand is vital to determine the suitability of the chemicals to prevent swelling. Table 2 shows the results of the minerals present in the sand sample, and Figure 4 shows the peaks for each mineral in the sample. Only quartz, sanidine (feldspar), and muscovite are present; hence, there will be no clay swelling that may affect the agglomeration mechanism.

3.2. Agglomeration Jar Test. The jar test was conducted based on the conditions generated from the DoE. Figure 5a shows the comparison between FO4290SH only and ChCl:U + FO4290SH. It can be seen that with the polymer only, the liquid is cloudy, but when the DES is added, the liquid becomes clear. Figure 5b shows some qualitative analysis of sand with ChCl:oxa, AN934SH, and FO4290SH. It can be seen that with only the DES, the liquid is cloudy, while with polymers, the sand has agglomerated and settled at the bottom and a clear solution can be seen. Analysis for baseline conditions is shown in Table 3.

As shown in Figure 6a, with NaCl brine, the glycerol DES performed better with the anionic polymer, while the urea DES and the oxalic acid DES performed better with the cationic polymer. As shown in Figure 6b, with $MgCl_2$ brine, the performances were similar for the glycerol DES and the urea DES in an anionic polymer, while the oxalic acid DES performed the best with a cationic polymer. As shown in Figure 6c, the best combination of the DES/polymer was used for analysis. The oxalic acid DES with a cationic polymer in both brines performed the best. Hence, it can be said that the oxalic acid DES had the biggest sand size, while the urea DES did not perform well in terms of the agglomeration size.

As shown in Figure 7a, the ideal zeta potential for agglomeration is between ±5 mV. Generally, the divalent ions will cause the zeta potential to decrease more due to the greater ionic strength.[33,34] In NaCl brine, the oxalic acid DES in both polymers achieved that range followed by the glycerol DES in the anionic polymer. As shown in Figure 7b, with $MgCl_2$ brine, the oxalic acid DES in both polymers achieved that range, while the glycerol DES in the anionic polymer had a bigger range. As shown in Figure 7c, the oxalic acid DES in the cationic polymer achieved that range in both brines, followed by the glycerol DES in both brines. Hence, it can be said that the oxalic acid DES can create the ideal condition for agglomeration.

Table 4. ANOVA of the Particle Size with ChCl:Oxalic Acid

source	sum of squares	df	mean square	F-value	p-value
model	39671.32	9	4407.92	30.98	0.0002
A-brine	4589.05	1	4589.05	32.25	0.0013
B-DES conc	5883.27	1	5883.27	41.35	0.0007
C-polymer conc	2356.86	1	2356.86	16.57	0.0066
E-temp	878.68	1	878.68	6.18	0.0475
F-polymer type	16951.39	1	16951.39	119.14	<0.0001
AB	1965.37	1	1965.37	13.81	0.0099
AE	1294.02	1	1294.02	9.1	0.0235
AF	3765.97	1	3765.97	26.47	0.0021
BF	1986.71	1	1986.71	13.96	0.0097
std. dev.	11.93		R^2	0.9789	
mean	248.98		adjusted R^2	0.9473	
C.V.%	4.79		predicted R^2	0.8502	
			adeq precision	20.054	

Table 5. ANOVA of the Zeta Potential with ChCl:Oxalic Acid

source	sum of squares	df	mean square	F-value	p-value
model	7.69	7	1.1	21.04	0.0001
A-brine	2.84	1	2.84	54.39	<0.0001
B-DES conc	0.3481	1	0.3481	6.67	0.0325
D-polymer dosage	0.8281	1	0.8281	15.86	0.004
AC	0.8649	1	0.8649	16.57	0.0036
AE	1.11	1	1.11	21.32	0.0017
BD	0.429	1	0.429	8.22	0.0209
BF	1.27	1	1.27	24.25	0.0012
std. dev.	0.2285		R^2	0.9485	
mean	−1.52		adjusted R^2	0.9034	
C.V.%	15.04		predicted R^2	0.7939	
			adeq precision	13.7264	
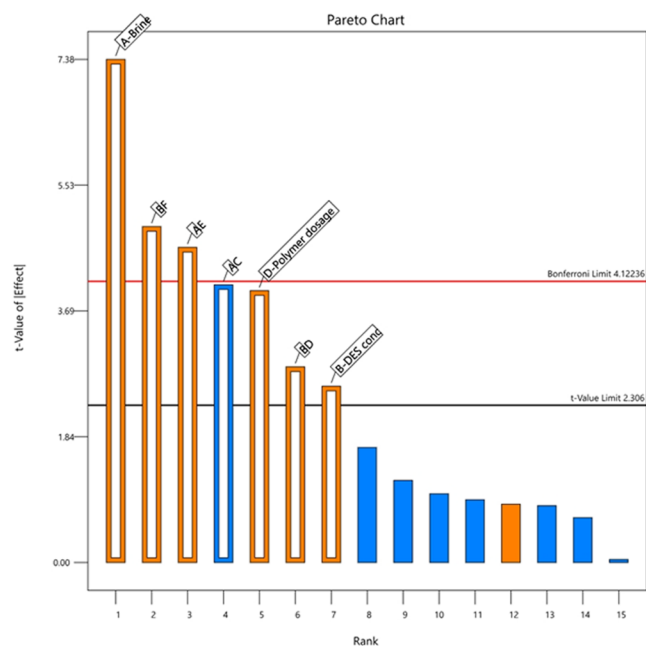
Figure 11. Pareto chart of the zeta potential for ChCl:oxalic acid.

Figure 12. Predicted vs actual values of the zeta potential of ChCl:oxalic acid.

Therefore, after considering both responses, the urea DES and the glycerol DES were eliminated from further optimization due to their performance compared to that of the oxalic acid DES.

3.3. RSM Analysis. In this experiment, the 2^6 fractional factorial was utilized to create 16 runs for each kind of DES, totaling 48 runs in all. The program then presented an ANOVA table to validate the degree of significance of each variable in connection to the responding variable, as well as the correlation coefficient, R^2, to demonstrate the confidence level of the analysis.[30−32] Following that, the program created an equation based on the variables, which was then used to optimize the optimum parameter combination to obtain the best outcomes. Finally, numerical optimization was used to obtain solutions for the optimal parameters.

After all of the results have been input into the table, the next step was the analysis. The software does not recommend any transformation for the model; hence, a linear model was applied. The fit statistics are shown in Figures 8, 9, 10, 12, and 13, while the ANOVA tables for the particle size and zeta potential are shown in Tables 4 and 5. The fit statistics show the fitting of the model where the adjusted R^2 should be near 0.9 to show good fitting and the difference between the
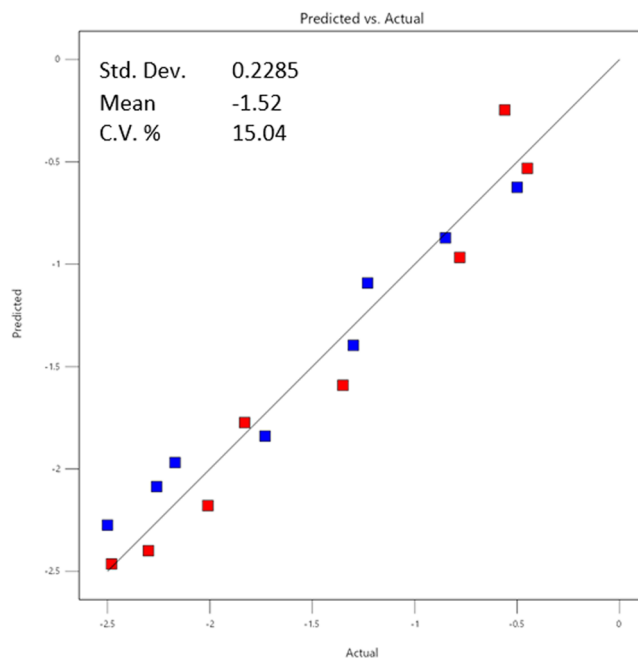
adjusted and predicted R^2 should not exceed 0.2. The ANOVA table shows the p-value of each parameter, where a p-value of below 0.05 indicates that it has a good relationship with the model (Tables 4 and 5).

Figure 8 shows the Pareto chart for the particle size; the factors above the Bonferroni limit (red line) and the t-value limit (black line) are significant for the model. Hence, factors A, B, C, E, F, AB, AE, AF, and BF were chosen for the modeling for the particle size. Figure 11 shows the Pareto chart for the zeta potential; factors A, B, C, D, AC, BD, and BF were chosen for the modeling.

As can be seen from Table 4, the p-values for the selected factors were below 0.05, which means that they were all significant toward the modeling. The difference between the adjusted and predicted R^2 is 0.09, which proves that the model is significant. As shown in Figure 9, the predicted vs actual values are near to the line, which means the difference in predictions are small. As shown in Figure 10, the residuals are around ±4, which means the analysis has a low error. In this case, factors A, B, C, E, F, AB, AE, AF, and BF are used in the
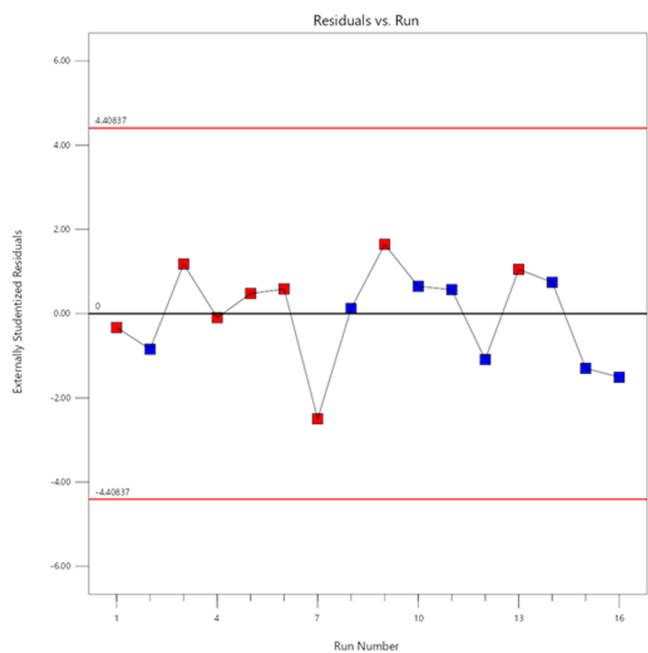
Figure 13. Residual vs run values of the zeta potential of ChCl:oxalic acid.

$$size = 248.98 + 16.94A + 19.18B - 12.14C - 7.41E$$
$$+ 32.55F - 11.08AB + 8.99AE - 15.34AF$$
$$+ 11.14BF \qquad (1)$$

As can be seen from Table 5, the p-values for the selected factors were below 0.05, which means that they were all significant toward the modeling. The difference between the adjusted and predicted R^2 is 0.11, which proves that the model is significant. As shown in Figure 14, the predicted vs actual values are near to the line, which means that the difference in predictions is small. As shown in Figure 15, the residuals are around ±4, which means that the analysis has a low error. In this case, factors A, B, C, D, AC, BD, and BF are used in the equation. The brine will be NaCl and the polymer will be cationic for standardization. The final equation will be as follows

$$zeta = -1.52 + 0.421A + 0.148B + 0.228D - 0.233AC$$
$$+ 0.264AE + 0.164BD + 0.281BF \qquad (2)$$

3.4. Optimization. After the analysis, optimizations were done by analyzing the interaction plots to show the effects of each variable on each response. The numerical optimization was used for targeted values of the responses, with a number of solutions available to show the best results.

As shown in Figure 14, the particle size was affected the most by the DES concentration and the polymer type. To achieve a high particle size indicated, the polymer used is cationic, the polymer concentration should be above 500 ppm, the DES concentration should be above 10000 ppm, and the
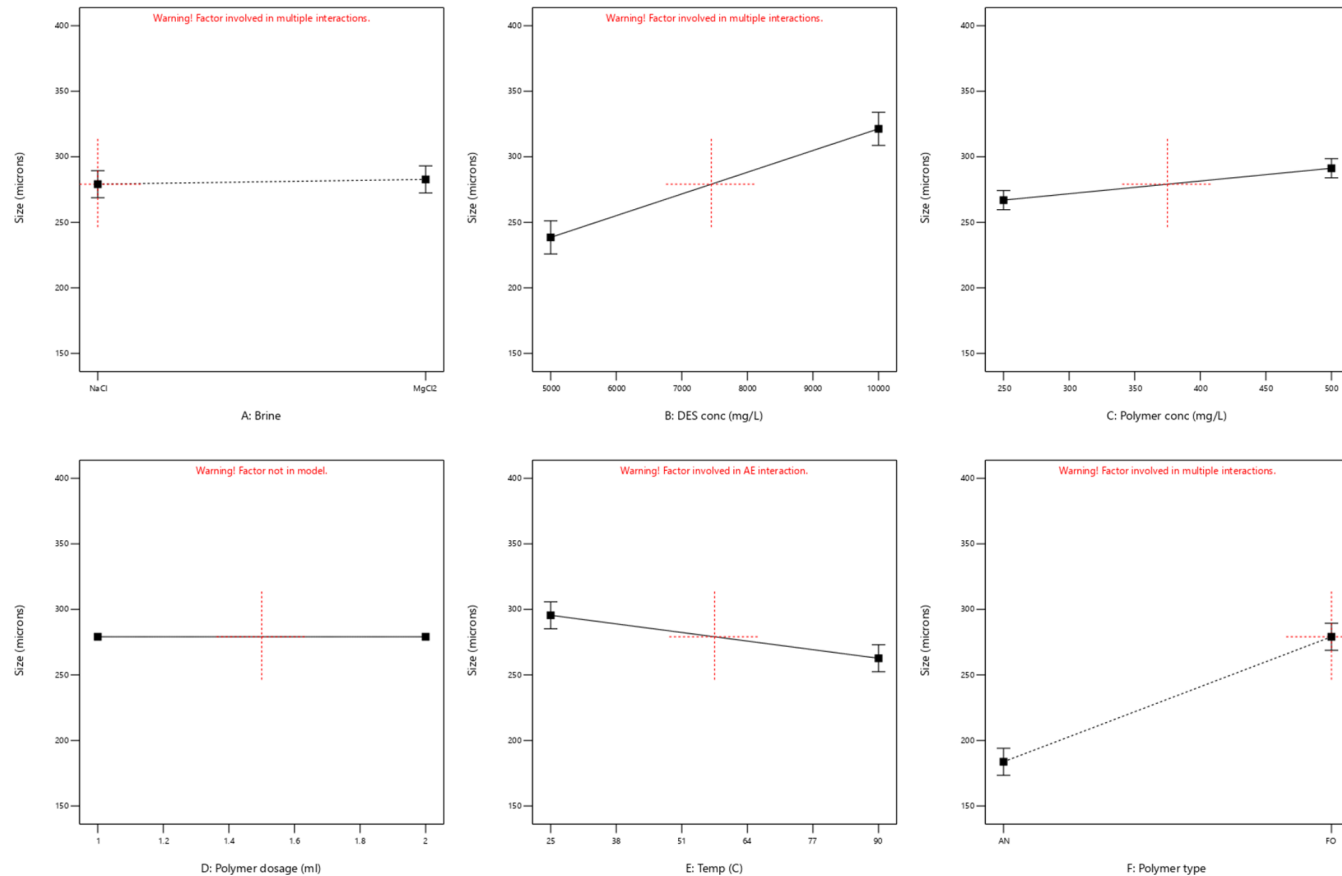
equation. The brine will be NaCl and the polymer will be cationic. The final equation will be as follows

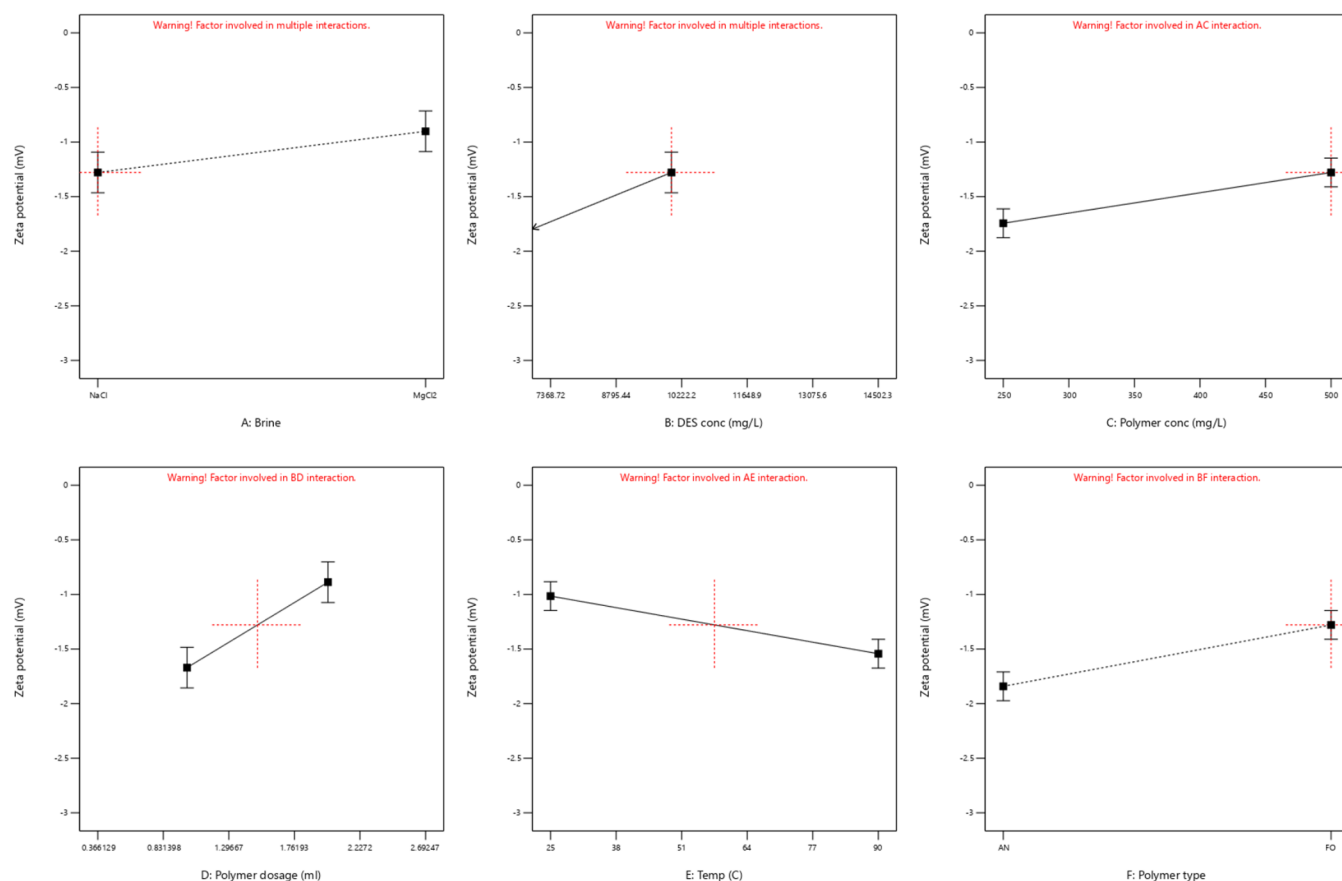**Figure 14.** Interaction plots of the particle size for ChCl:oxalic acid.

Figure 15. Interaction plots of the zeta potential for ChCl:oxalic acid.

Table 6. Constraints for Numerical Optimization

name	goal	lower limit	upper limit	lower weight	upper weight	importance
A-brine	is equal to NaCl	NaCl	MgCl2	1	1	3
B-DES conc.	maximize	5000	15000	1	1	5
C-polymer conc.	maximize	250	1000	1	1	5
D-polymer dosage	maximize	1	4	1	1	5
E-temp	maximize	25	100	1	1	5
F-polymer type	is equal to FO	AN	FO	1	1	3
size	is target = 350	300	358.7	1	1	5

Table 7. Proposed Solutions and Percentage Error

no.	brine	DES conc. (ppm)	polymer conc. (ppm)	polymer dosage (mL)	temp (°C)	polymer type	size (μm)	zeta potential (mV)
1	NaCl	10656.48	779.134	2.124	100	FO	predicted: 349.99 actual: 353.75 error: 1.07%	predicted: −0.45 actual: −0.78 error: 73.3%
2	NaCl	10656.55	779.119	2.124	100	FO	predicted: 349.99 actual: 352.68 error: 0.76%	predicted: −0.45 actual: −0.65 error: 44.4%

temperature can be varied. As shown in Figure 15, the zeta potential was affected by all 6 factors. To achieve a zeta potential of less than −1 mV, the polymer used is cationic, the brine type should be NaCl, the DES concentration should be above 10 000 ppm, the polymer concentration should be above 500 ppm, and the polymer dosage should be greater than 2 mL.

After the interaction analysis, numerical optimization was used, as shown in Table 6. The brine is NaCl, the polymer type is cationic, the DES concentration is maximized between 5000

and 15000 ppm, the polymer concentration is maximized between 250 and 1000 ppm, the polymer dosage is maximized between 1 and 4 mL, and the temperature is maximized between 25 and 100 °C. The proposed solutions are then tested for the percentage error.

The proposed solutions together with the percentage error are shown in Table 7. The particle size obtained was consistent, with an error around 1%. The zeta potential was also consistent, and despite the large percentage error imposed, the actual difference between the values was small.

4. CONCLUSIONS

The pairing of deep eutectic solvents with ionic polymers as a sand-agglomerating chemical has not been previously reported for usage in the oil and gas industry. The factors investigated, which are the type of brine, type of DES, DES concentration, polymer concentration, polymer dosage, and temperature, are all significant toward understanding their interaction. It was shown that ChCl:urea performed the worst, and ChCl:oxalic acid was the most effective. For it to achieve a high particle size and a zeta potential range of near 0 mV, it was shown that a divalent salt such as $MgCl_2$ brine can decrease the zeta potential more, the DES concentration should be above 10 000 ppm, the polymer should be cationic, the concentration should be around 800 ppm, the dosage can be around 2−3 mL, and the temperature can be up to 100 °C. The use of DOE software is highly accurate and can process the analysis without the need to perform all possible combinations. The most suitable combinations based on the given data were generated and tested; the difference in values is not high, which proves that the DOE is accurate in its predictions.

AUTHOR INFORMATION

Corresponding Author

Angelov Tan Yew Ming − *Department of Petroleum Engineering, Universiti Teknologi Petronas, 32610 Seri Iskandar, Perak, Malaysia;* orcid.org/0009-0004-1452-4152; Email: angelov_22009986@utp.edu.my

Authors

Iskandar bin Dzulkarnain − *Department of Petroleum Engineering, Universiti Teknologi Petronas, 32610 Seri Iskandar, Perak, Malaysia; Centre of Research in Enhanced Oil Recovery, Institute of Hydrocarbon Recovery, Universiti Teknologi Petronas, 32610 Seri Iskandar, Perak, Malaysia*

Syahrir Ridha − *Department of Petroleum Engineering, Universiti Teknologi Petronas, 32610 Seri Iskandar, Perak, Malaysia; Centre of Research in Enhanced Oil Recovery, Institute of Hydrocarbon Recovery, Universiti Teknologi Petronas, 32610 Seri Iskandar, Perak, Malaysia*

Complete contact information is available at:
https://pubs.acs.org/10.1021/acsomega.4c03759

Notes

The authors declare no competing financial interest.

REFERENCES

(1) Karimi, S.; Shirazi, S. A.; McLaury, B. S. Predicting Fine Particle Erosion Utilizing Computational Fluid Dynamics. *Wear* **2017**, *376−377*, 1130−1137.

(2) Varga, M.; Goniva, C.; Adam, K.; Badisch, E. Combined Experimental and Numerical Approach for Wear Prediction in Feed Pipes. *Tribol. Int.* **2013**, *65*, 200−206.

(3) Dees, J. M. Sand Control in Wells With Gas Generator and Resin. In *SPE Annual Technical Conference and Exhibition*; SPE: Washington DC, 1992.

(4) Tabbakhzadeh, M. N.; Esmaeilzadeh, F.; Zabihi, R.; Mowla, D. Experimental Study of Chemical Sand Consolidation Using Epoxy and Furan Resins for Oil Wells: Experimental Design Models. *Int. J. Rock Mech. Min. Sci.* **2020**, *135*, No. 104486.

(5) Ogbebor, L. O.; Nmakwe, C. M. A Study of pH and Zeta Potential of Nanoparticle Transport in Porous Media. 2019, *4* (12).

(6) Fauzi, N. A. M.; Ganat, T. A.; Elraies, K. A.; Ridha, S.; Zainal, S.; Saphanuchart, W. Agglomeration of Fines and Sand in the Separator. In *Day 1 Mon, November 02, 2020*; OTC: Kuala Lumpur, Malaysia, 2020; p D012S001R087.

(7) Sultana, K.; Rahman, M. T.; Habib, K.; Das, L. Recent Advances in Deep Eutectic Solvents as Shale Swelling Inhibitors: A Comprehensive Review. *ACS Omega* **2022**, *7* (33), 28723−28755.

(8) Lee, R. Y. Development of Sand Agglomeration Formulation for Oil and Gas Well Applications to Reduce the Production of Fine Particulates, Doctoral Dissertation, 2019.

(9) Lahalih, S. M.; Ghloum, E. F. Rheological Properties of New Polymer Compositions for Sand Consolidation and Water Shutoff in Oil Wells. *J. Appl. Polym. Sci.* **2007**, *104* (4), 2076−2087.

(10) Marandi, S. Z.; Salehi, M. B.; Moghadam, A. M. Sand Control: Experimental Performance of Polyacrylamide Hydrogels. *J. Pet. Sci. Eng.* **2018**, *170*, 430−439.

(11) Al-Risheq, D. I. M.; Nasser, M. S.; Qiblawey, H.; Hussein, I. A.; Benamor, A. Choline Chloride Based Natural Deep Eutectic Solvent for Destabilization and Separation of Stable Colloidal Dispersions. *Sep. Purif. Technol.* **2021**, *255*, No. 117737.

(12) I M Al-Risheq, D.; Shaikh, S. M. R.; Nasser, M. S.; Almomani, F.; Hussein, I. A.; Hassan, M. K. Influence of Combined Natural Deep Eutectic Solvent and Polyacrylamide on the Flocculation and Rheological Behaviors of Bentonite Dispersion. *Sep. Purif. Technol.* **2022**, *293*, No. 121109.

(13) Haz, A.; Strizincova, P.; Majova, V.; Skulcova, A.; Jablonsky, M. Thermal Stability of Selected Deep Eutectic Solvents. *Int. J. Sci. Res.* **2016**, *7*, 14441−14444.

(14) Delgado-Mellado, N.; Larriba, M.; Navarro, P.; Rigual, V.; Ayuso, M.; García, J.; Rodríguez, F. Thermal Stability of Choline Chloride Deep Eutectic Solvents by TGA/FTIR-ATR Analysis. *J. Mol. Liq.* **2018**, *260*, 37−43.

(15) Ma, J.; Pang, S.; Zhou, W.; Xia, B.; An, Y. Novel Deep Eutectic Solvents for Stabilizing Clay and Inhibiting Shale Hydration. *Energy Fuels* **2021**, *35* (9), 7833−7843.

(16) Abdulnabi, A.; Amoako, K.; Moran, D.; Vanadara, K.; Aldaeef, A. A.; Esmaeilzadeh, A.; Beier, N.; Soares, J.; Simms, P. Evaluation of Candidate Polymers to Maximize Geotechnical Performance of Oil Sands Tailings. *Can. Geotech. J.* **2022**, *59* (3), 359−371.

(17) Cunha, S. C.; Fernandes, J. O. Extraction Techniques with Deep Eutectic Solvents. *TrAC Trends Anal. Chem.* **2018**, *105*, 225−239.

(18) Chabib, C. M.; Ali, J. K.; Jaoude, M. A.; Alhseinat, E.; Adeyemi, I. A.; Al Nashef, I. M. Application of Deep Eutectic Solvents in Water Treatment Processes: A Review. *J. Water Process Eng.* **2022**, *47*, No. 102663.

(19) Huang, H.; Babadagli, T.; Chen, X.; Andy Li, H. Performance Comparison of Novel Chemical Agents in Improving Oil Recovery from Tight Sands through Spontaneous Imbibition. *Pet. Sci.* **2020**, *17* (2), 409−418.

(20) Mohsenzadeh, A.; Al-Wahaibi, Y.; Al-Hajri, R.; Jibril, B.; Joshi, S.; Pracejus, B. Investigation of Formation Damage by Deep Eutectic Solvents as New EOR Agents. *J. Pet. Sci. Eng.* **2015**, *129*, 130−136.

(21) Mohsenzadeh, A.; Al-Wahaibi, Y.; Jibril, A.; Al-Hajri, R.; Shuwa, S. The Novel Use of Deep Eutectic Solvents for Enhancing Heavy Oil Recovery. *J. Pet. Sci. Eng.* **2015**, *130*, 6−15.

(22) Juneidi, I.; Hayyan, M.; Hashim, M. A. Evaluation of Toxicity and Biodegradability for Cholinium-Based Deep Eutectic Solvents. *RSC Adv.* **2015**, *5* (102), 83636−83647.

(23) Abbott, A. P.; Capper, G.; Davies, D. L.; Rasheed, R. K.; Tambyrajah, V. Novel Solvent Properties of Choline Chloride/Urea Mixtures. *Chem. Commun.* **2003**, *1*, 70−71.

(24) Abbott, A. P.; Boothby, D.; Capper, G.; Davies, D. L.; Rasheed, R. K. Deep Eutectic Solvents Formed between Choline Chloride and Carboxylic Acids: Versatile Alternatives to Ionic Liquids. *J. Am. Chem. Soc.* **2004**, *126* (29), 9142−9147.

(25) Rasool, M. H.; Zamir, A.; Elraies, K. A.; Ahmad, M.; Ayoub, M.; Abbas, M. A. A Deep Eutectic Solvent Based Novel Drilling Mud with Modified Rheology for Hydrates Inhibition in Deep Water Drilling. *J. Pet. Sci. Eng.* **2022**, *211*, No. 110151.

(26) Luo, Z.; Wang, L.; Yu, P.; Chen, Z. Experimental Study on the Application of an Ionic Liquid as a Shale Inhibitor and Inhibitive Mechanism. *Appl. Clay Sci.* **2017**, *150*, 267−274.

(27) Benzagouta, M. S.; AlNashef, I. M.; Karnanda, W.; Al-Khidir, K. Ionic Liquids as Novel Surfactants for Potential Use in Enhanced Oil Recovery. *Korean J. Chem. Eng.* **2013**, *30* (11), 2108−2117.

(28) Ma, J.; Pang, S.; Zhou, W.; Xia, B.; An, Y. Novel Deep Eutectic Solvents for Stabilizing Clay and Inhibiting Shale Hydration. *Energy Fuels* **2021**, *35* (9), 7833−7843.

(29) Tomé, L. I.; Baião, V.; Da Silva, W.; Brett, C. M. A. Deep Eutectic Solvents for the Production and Application of New Materials. *Appl. Mater. Today* **2018**, *10*, 30−50.

(30) He, J.; Zhu, L.; Liu, C.; Bai, Q. Optimization of the Oil Agglomeration for High-Ash Content Coal Slime Based on Design and Analysis of Response Surface Methodology (RSM). *Fuel* **2019**, *254*, No. 115560.

(31) Shahsavari, M. H.; Khamehchi, E. Optimum Selection of Sand Control Method Using a Combination of MCDM and DOE Techniques. *J. Pet. Sci. Eng.* **2018**, *171*, 229−241.

(32) Yadav, A. M.; Nikkam, S.; Gajbhiye, P.; Tyeb, M. H. Modeling and Optimization of Coal Oil Agglomeration Using Response Surface Methodology and Artificial Neural Network Approaches. *Int. J. Miner. Process.* **2017**, *163*, 55−63.

(33) Vinogradov, J.; Jackson, M. D.; Chamerois, M. Zeta Potential in Sandpacks: Effect of Temperature, Electrolyte pH, Ionic Strength and Divalent Cations. *Colloids Surf. Physicochem. Eng. Asp.* **2018**, *553*, 259−271.

(34) Nasralla, R. A.; Nasr-El-Din, H. A. Impact of Cation Type and Concentration in Injected Brine on Oil Recovery in Sandstone Reservoirs. *J. Pet. Sci. Eng.* **2014**, *122*, 384−395.